catalysts

MDPI

Article

A Green Route to Methyl Formate from CO_2-Derived Formamides over Solid Base Catalysts

Xin He, Xu Guo, Guofu Xia *, Run Xu, Yu Wu and Xuebin Luan

SINOPEC Research Institute of Petroleum Processing Co., Ltd., Beijing 100083, China
* Correspondence: xiaguofu.ripp@sinopec.com

Abstract: The transformation of CO_2 and CO_2-derived chemicals into high value-added chemicals is an important method for reducing CO_2 emissions and achieving carbon neutrality. Methyl formate (MF) is a critical C1 building block in synthesizing a wide range of important chemicals, such as formic acid, ethylene glycol, and formamide methyl propionate. Here, we report a green route for the sustainable synthesis of MF from CO_2-derived formamides via the alcoholysis reaction catalyzed by supported CaO solid bases. The CaO/MgO catalyst with 13.5 wt.% CaO exhibited higher alcoholysis reaction efficiency and achieved 94.5% conversion of N-formylmorpholine and 100% selectivity of MF in methanol at 120 °C. Based on the kinetic studies, characterization results of structural and basic properties (XRD, and TEM, CO_2-TPD, etc.), we found that the density of strong basic sites is linearly related to the activity of alcoholysis reaction, and the higher the base density on these catalysts, the greater the reaction rate. This study presents a sustainable route for the synthesis of MF by using CO_2-derived formamides and green methanol, and a promising strategy for producing more efficient solid alcoholysis catalysts of amides.

Keywords: methyl formate; solid base catalyst; formamides alcoholysis; CaO/MgO

check for updates

Citation: He, X.; Guo, X.; Xia, G.; Xu, R.; Wu, Y.; Luan, X. A Green Route to Methyl Formate from CO_2-Derived Formamides over Solid Base Catalysts. *Catalysts* **2023**, *13*, 487. https://doi.org/10.3390/catal13030487

Academic Editors: Xin Jin, Daming Gao and Raghunath Vitthal Chaudhari

Received: 28 December 2022
Revised: 20 January 2023
Accepted: 31 January 2023
Published: 28 February 2023

Copyright: © 2023 by the authors. Licensee MDPI, Basel, Switzerland. This article is an open access article distributed under the terms and conditions of the Creative Commons Attribution (CC BY) license (https://creativecommons.org/licenses/by/4.0/).

1. Introduction

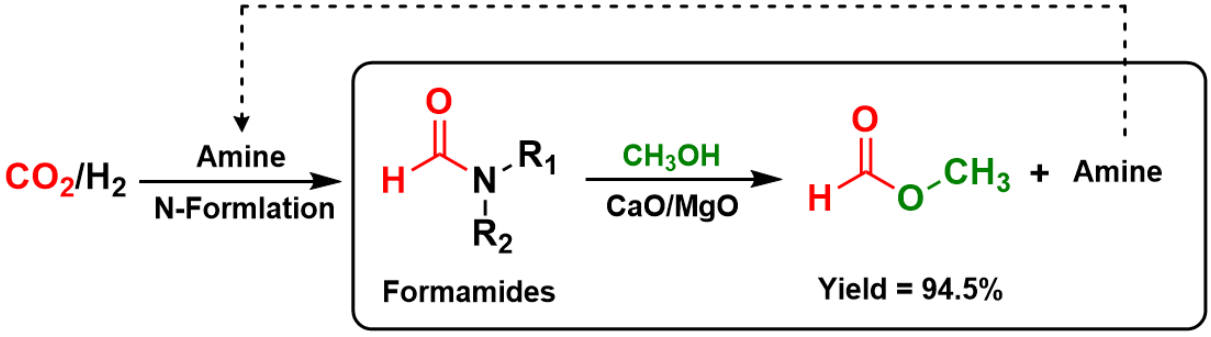
Methyl formate (MF) is a fundamental C1 building block for manufacturing a wide range of critical chemicals, such as formic acid, ethylene glycol, and formamide methyl propionate [1]. MF could well be thermally degraded to CO, making it a safe carbonylation source to substitute for CO. Methanol carbonylation [2,3] and methanol dehydrogenation [4,5] are the primary industrial processes for MF synthesis. Methanol carbonylation utilizes methanol and CO as raw materials to produce MF with the advantage of high product selectivity. However, due to the utilization of a homogeneous basic catalyst (sodium methylate), this process is challenging to run continuously, and the catalyst is readily deactivated. Methanol dehydrogenation is catalyzed by supported copper-based heterogeneous catalysts, which have excellent catalyst stability under mild reaction conditions with simple feedstocks. However, the selectivity of MF is low and the methanol conversion is limited by thermodynamics. With the expansion of the downstream industry, the need for MF is expected to increase continuously. Therefore, it is urgent to develop a green and efficient MF production process.

The transformation of CO_2 and CO_2-derived chemicals into chemicals with high value-added is a creative strategy for both reducing CO_2 emissions and achieving carbon neutrality [6–8]. One intriguing approach to fix CO_2 is the synthesis of formamides through N-formylation of amines using CO_2 and H_2, which has been achieved over homogeneous ($RuCl_2(P(CH_3)_3)_4$ [9,10], $RuCl_2(dppe)_2$ [11] and other Ru complexes [12,13]), and heterogeneous catalysts (Pd/Al_2O_3 [14], Pd/C [15], Pd@POPs [16], Cu/ZnO [17], and Ir/TiO_2 [18], etc.). The yield of N-formylmorpholine (NFM) from the N-formalation reaction of CO_2, H_2, and morpholine on various catalyst systems exceeds 95% at mild reaction conditions, making NFM a CO_2-derived green chemical. Therefore, developing

new utilization pathways for CO_2-derived formamides can greatly expand the CO_2 transformation and facilitate the sustainable development of green synthesis for potential high value-added chemicals.

Alcoholysis is an effective method for converting formamides or amides to esters and amines [19–23]. These studies have demonstrated that both formamides and amides can be alcoholized over basic catalysts even though the amide bond is relatively stable. Li et al. used a homogeneous Cs_2CO_3 catalyst to convert formamides to MF and amines in methanol, and the yield of MF reached almost 100% [21]. Deguchi et al. reported the catalytic alcoholysis of 8-aminoquinoline amides over air-stable homogeneous Ni complexes catalysts at 80 °C [22]. Although these homogeneous catalysts are effective in catalyzing alcoholysis reactions, they are more costly to separate and difficult to apply in continuous industrial processes. However, heterogeneous catalysts for the alcoholysis of amides are poorly reported. To the best of our knowledge, there is only one report on reusable catalysts for the alcoholysis of amide to the corresponding ester from Siddiki et al. [23]. They utilized heterogeneous CeO_2 to convert amides and alcohols toward esters with more than 90% yield, but the reaction occurred under a harsh condition (165 °C) and the substrates were limited to amides where the amino group was not substituted with other groups. In order to achieve highly efficient alcoholysis of amides and industrialization of the process, heterogeneous alcoholysis catalysts with more activity and wider adaptability still need to be developed urgently.

Calcium oxide is a typical solid base catalyst, which is widely employed in the preparation of biodiesel by alcoholysis of fats [24,25], the synthesis of glycerol carbonate from glycerol [26], and other high value-added chemicals via ether elimination reactions [27]. Although calcium oxide has excellent alkaline catalytic activity, the high-temperature calcination in the preparation of bulk calcium oxide results in a low specific surface area, which in turn limits its mass activity. Thus, it is an effective way to increase the dispersion and boost the catalytic reactivity of calcium oxide by embedding it onto suitable supports. In this study, we report a green route for the sustainable synthesis of MF from CO_2-derived formamides via an alcoholysis reaction catalyzed by supported CaO solid bases in green methanol (Scheme 1), which contributes to the utilization of CO_2 and production of high value-added and sustainable green chemicals. The CaO/MgO catalyst with 13.5 wt.% CaO exhibited excellent alcoholysis reaction efficiency with 94.5% conversion of NFM and 100% selectivity of MF in methanol at 120 °C. Notably, the typical basic sites on CaO/MgO catalysts facilitated the alcoholysis reaction of amides. The by-product amine can be recycled for the synthesis of formamides with CO_2 and H_2 by N-formylation reaction, showing the excellent atom economy of this process.



Scheme 1. Scheme of the alcoholysis reaction of formamides to methyl formate and amine.

2. Results and Discussion

Alkaline catalysts are often used in the alcoholysis of esters, which provides inspiration for the study of the alcoholysis of amides. Several solid base catalysts were screened in methanol at 120 °C for the alcoholysis reaction of NFM to MF and morpholine. Table 1 lists the initial rate of catalysts at ca. 30% conversion of NFM. The reaction of NFM in the

absence of any catalysts was completely inactive for the MF formation (Entry 1). MgO, $Ca_5(PO_4)_3OH$, and Na_2CO_3 were poorly active in the alcoholysis reaction of NFM (0.016, 0.026, and 0.037 mmol·g^{-1}·h^{-1}, respectively); although, the selectivities of the products reached 100% (Entries 2–4). On CeO_2 and Hydrotalcite, the alcoholysis rates were 0.042 and 0.053 mmol·g^{-1}·h^{-1}, respectively, whereas the selectivities of MF and morpholine did not exceed 90% (entries 5, 6). It is suggested that the ring-opening reaction of morpholine and other side reactions may be responsible for the decreased selectivities of products on these two catalysts. Compared with the above solid bases, the CaO catalyst showed an excellent efficiency for alcoholysis reaction with a 0.178 mmol·g^{-1}·h^{-1} reaction rate and 100% MF selectivity (Entry 7). Thus, CaO is the preferable catalyst for the alcoholysis reaction of NFM to MF.

Table 1. Reaction rate and product selectivities of NFM alcoholysis reaction over different solid base catalysts.

Entry	Catalyst	Rate (mmol·g^{-1}·h^{-1})	Molar Selectivity (%)	
			MF	Morpholine
1	Blank	0	-	-
2	MgO	0.016	100	100
3	$Ca_5(PO_4)_3OH$	0.026	100	100
4	Na_2CO_3	0.037	100	100
5	CeO_2	0.042	68	83
6	Hydrotalcite	0.053	79	89
7	CaO	0.178	100	100

Reaction conditions: 120 °C, 0.3 g catalyst, 1.0 mmol NFM, 15 mL methanol, ~30% NFM conversion controlled by reaction time.

However, the specific surface area of CaO is rather modest (10.8 m^2·g^{-1}, shown in Table 2), which is the primary factor for its limitation in catalytic reactivity. Compared with increasing catalyst feed or amplifying the specific surface area, loading highly dispersed CaO species on catalyst supports is an effective strategy for improving both the catalytic activity and utilization efficiency. Thus, a series of supported CaO/MgO catalysts with varied CaO content was produced to transform NMF to MF and morpholine. BET surface area of the as-synthesized catalysts improved from 26.3 to 34.9 m^2·g^{-1} with the increment of MgO content (Table 2). Figure 1 shows that no excess diffraction peaks appear in the powder XRD spectra of CaO/MgO catalysts except diffraction peaks of CaO (PDF#48-1467) and MgO (PDF#45-0946), indicating that CaO and MgO did not form new crystalline phases in CaO/MgO catalysts. In addition, the diffraction peak intensity of CaO in CaO/MgO catalysts gradually improved with the increase in CaO content. The average particle sizes of 3.8% CaO/MgO, 7.2% CaO/MgO, 10.5% CaO/MgO, 13.5% CaO/MgO, 16.3% CaO/MgO, and CaO are 42.5, 42.7, 43.5, 48.3, 55.4, and 83.1 nm, respectively, as calculated by the Scherrer equation based on the powder XRD spectra. The much smaller particle size of supported CaO compared to bulk CaO reveals that MgO can effectively increase the dispersion of CaO.

The uniform distribution of CaO on MgO was verified by the TEM (Figure 2a) and the EDS mapping (Figure 2b). The lattice fringes on the crystalline surfaces of CaO(111) and MgO(200) (lattice spacing of 0.278 nm and 0.210 nm, respectively) are clearly visible in the high-resolution TEM images of the 13.5% CaO/MgO. Taken together, the characterization results of XRD and TEM demonstrate that CaO can be well dispersed on the MgO support, which, in turn, increases the density of basic sites and the reactivity of the catalyst, as described below.

As shown in Table 2, the alcoholysis reaction of NFM to MF and morpholine occurred over supported CaO/MgO catalysts in the kinetically controlled regime (at ca. 30% conversion of NFM) under 120 °C. The alcoholysis rate of NFM over the 3.8% CaO/MgO catalyst was 0.12 mmol·g^{-1}·h^{-1} (Entry 2), which was about 7.5 times higher than the MgO catalyst (Entry 1). As the mass fraction of CaO increased from 3.8% to 13.5%, the alcoholysis rate of

NFM improved to 0.263 mmol·g^{-1}·h^{-1} (Entry 3–5), which was approximately 1.5 times higher than that of bulk CaO (Entry 8). The alcoholysis rate (0.261 mmol·g^{-1}·h^{-1}) remained essentially the same as the mass fraction content of CaO increased to 16.3% (Entry 6). The molar selectivities of both morpholine and MF remained 100%, which means that the products were stable on CaO/MgO catalysts under reaction conditions. Moreover, by comparing the alcoholysis rate of the mechanically mixed 13.5% CaO + MgO catalyst with the 13.5% CaO/MgO catalyst, the reaction rate of alcoholysis on the 13.5% CaO/MgO catalyst was significantly higher than that on the mechanically mixed one (0.045 mmol·g^{-1}·h^{-1}, Entry 7). Such a comparison reinforces that the impregnation process facilitated the dispersion of CaO and the reactivity of CaO/MgO catalysts.

Table 2. Alcoholysis rate of NFM and product selectivities over different CaO/MgO catalysts.

Entry	Catalyst	S_{BET} ($m^2 \cdot g^{-1}$)	Rate (mmol·g^{-1}·h^{-1})	Molar Selectivity (%)	
				MF	Morpholine
1	MgO	36.6	0.016	100	100
2	3.8% CaO/MgO	34.9	0.120	100	100
3	7.2% CaO/MgO	31.4	0.180	100	100
4	10.5% CaO/MgO	30.2	0.228	100	100
5	13.5% CaO/MgO	28.1	0.263	100	100
6	16.3% CaO/MgO	26.3	0.261	100	100
7	13.5% CaO + MgO [a]	-	0.045	100	100
8	CaO	10.8	0.178	100	100

Reaction conditions: 120 °C, 0.3 g catalyst, 1.0 mmol NFM, 15 mL methanol, ~30% NFM conversion controlled by reaction time. [a] The CaO and MgO were mechanically mixed with a mass ratio of 13.5%:86.5%.

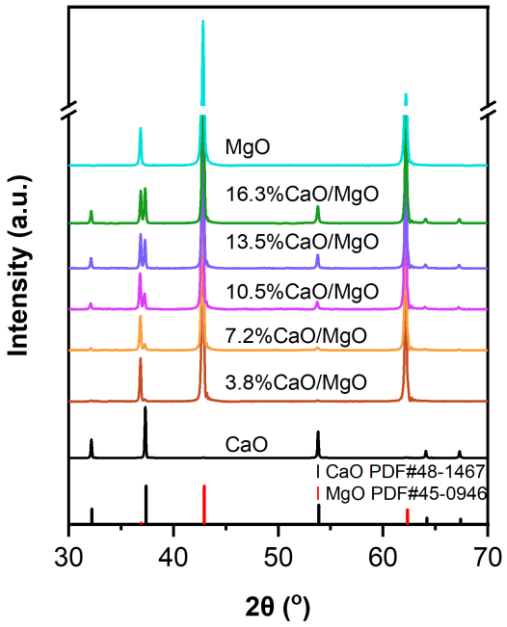


Figure 1. Powder XRD spectra of CaO, MgO, and CaO/MgO catalysts with different CaO mass fractions.

The identification of the active site of the catalyst is key to understanding the reaction mechanism. DFT calculations demonstrated that the strong base sites of CeO_2 are the most important factor for the high reactivity of the alcoholysis of amides [20]. The methanolysis reaction of amide is very similar to ester, both involving the breaking of the C-N or C-O bonds of the substrate and the activation of the O-H bonds of methanol. The mechanism of CaO-catalyzed methanolysis reactions of esters has been verified by numerous theoretical calculations and experimental results [28–30], and the basic sites are the catalytically active sites for this type of reaction. The methanolysis reaction of ester catalyzed by CaO initiated the formation of a methoxide anion via the abstraction of methanol's proton by

the highly catalytic active basic sites (conjugated oxygen anions) of CaO. The O-H bonds easily break to form methoxide anions and hydrogen cations. Next, the methoxide anion attacks (nucleophilic) the carbonyl carbon of ester and forms an alkoxycarbonyl tetrahedral intermediate. The unstable alkoxycarbonyl intermediate is then transformed into methyl carboxylate. In the last step, the formation of the corresponding fatty alcohols and the regeneration of CaO active sites occur. Based on the understanding of the mechanism of the CaO-catalyzed methanolysis reaction of ester, it is reasonable to believe that the strongly basic sites have a significant correlation with the activity of the amide alcoholysis reaction.

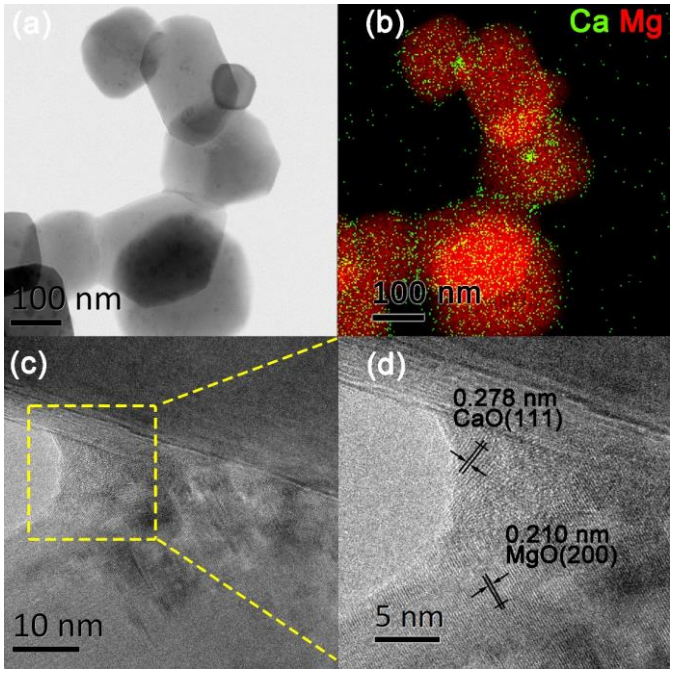


Figure 2. (**a**) TEM images, (**b**) EDS mapping images of Ca and Mg elements, and (**c**,**d**) high-resolution TEM images of 13.5% CaO/MgO.

The CO_2-TPD profiles of CaO, MgO, and various CaO/MgO catalysts are shown in Figure 3a. CaO and different CaO/MgO catalysts exhibit a characteristic CO_2 desorption peak at approximately 600 °C, which corresponded with strongly basic sites on these catalysts [31]. In contrast, the MgO catalyst just has a modest CO_2 desorption peak at about 200 °C, which echoes with the lower alcoholysis reactivity of MgO. According to the reaction results depicted in Table 2, the strong basic sites are suggested to be the intrinsic active species. To further verify this conjecture, the correlation between the density of strong basic sites and the reaction rates was investigated. As illustrated in Figure 3b, the kinetic analysis revealed that the basic density of the supported CaO catalysts increased with the increment of CaO content until it reached the plateau value (~0.50 $mmol_{base} \cdot g^{-1}$) on 13.5% CaO/MgO. The alcoholysis rate of NFM correlated linearly with the base density of these catalysts, and the TOF of NFM remained almost constant with the increment of the density of base sites. Thus, these two correlations strictly indicated that the strong basic sites are catalytic activity centers of both CaO and CaO/MgO catalysts.

The effect of temperature on the alcoholysis reaction of NFM over 13.5% CaO/MgO was examined (Figure 4a). As the temperature raised from 90 to 120 °C, the alcoholysis rate of NFM increased from 0.086 to 0.263 $mmol \cdot g^{-1} \cdot h^{-1}$, while the selectivity of morpholine and MF was maintained at 100%. Such a result elucidated that the temperature just exerted an effect on the reaction rate instead of the selectivity of products. Further analysis of the reaction rate versus temperature revealed that $ln(r)$ had a linear relationship with $1/T$ (as shown in Figure 4b). The apparent activation energy of the alcoholysis reaction on 13.5% CaO/MgO (44.6 kJ/mol) was calculated by using the Arrhenius equation, which is

essentially comparable with bulk CaO (45.5 kJ/mol). Combined with the kinetic studies on CaO-based catalysts, it is clear that the supported CaO and the bulk CaO share the same active sites for catalyzing the alcoholysis reaction of NFM.

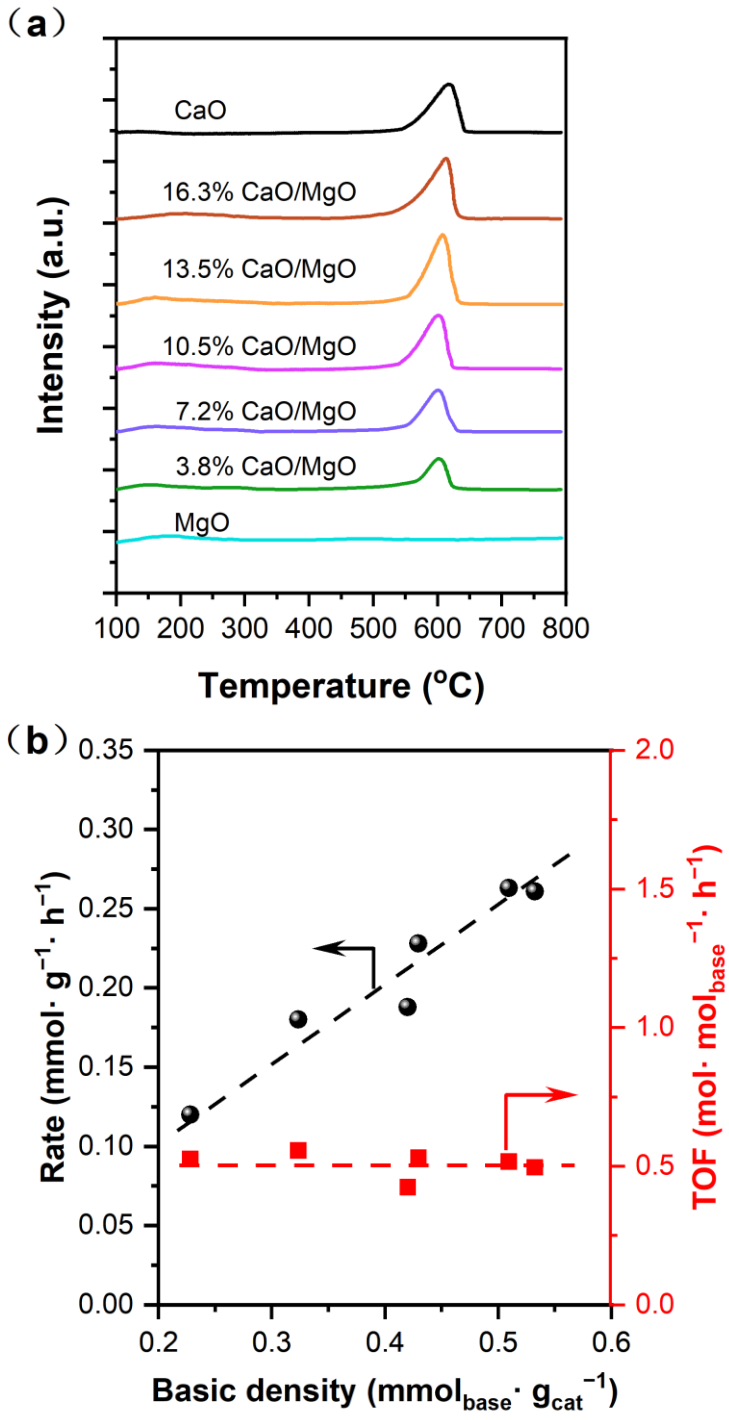


Figure 3. (**a**) CO_2-TPD profiles of CaO, MgO, and different CaO/MgO catalysts, (**b**) correlation of rate and TOF values with the basic density for CaO/MgO catalysts. Reaction conditions: 120 °C, 0.3 g catalyst, 1.0 mmol NFM, 15 mL methanol, ~30% NFM conversion controlled by reaction time.

The effect of reaction time on the conversion of NFM and product selectivities is shown in Figure 5. With the increase in reaction time, the conversion of NFM increased to 94.5%, but reached a plateau due to the decreased concentration of NFM in the later stage of the reaction. The selectivity of MF and morpholine remained stable at 100% independent with

the reactant conversion, indicating that MF and morpholine are primary products of the alcoholysis reaction and these products could remain stable under such a reaction condition.

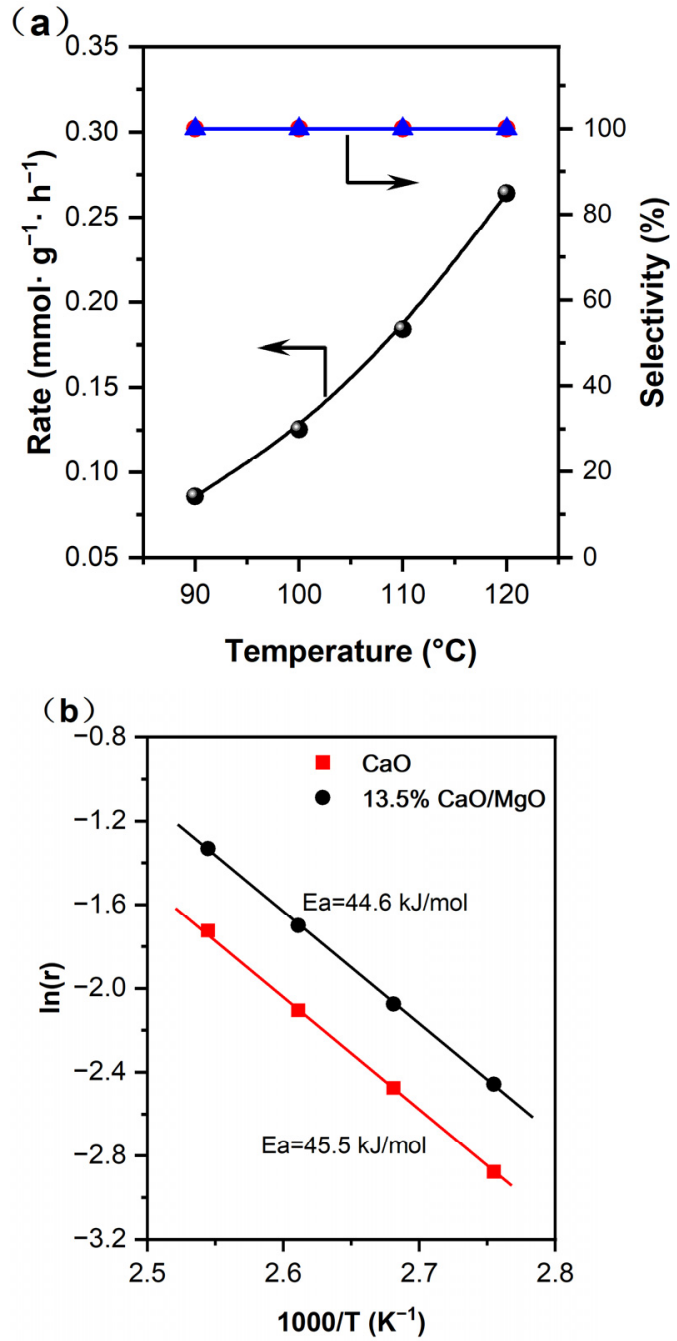


Figure 4. (**a**) The effect of temperature on the alcoholysis rate of NFM and product selectivities, (**b**) the relationship between $ln(r)$ and $1/T$ in the NFM alcoholysis reaction on 13.5% CaO/MgO. Reaction conditions: 0.3 g catalyst, 1.0 mmol NFM, 15 mL methanol, around 30% NFM conversion controlled by reaction time.

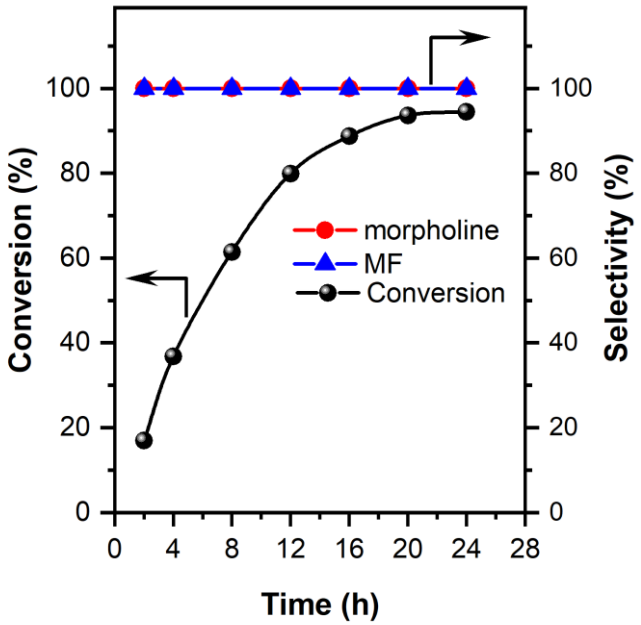


Figure 5. The effect of reaction time on the conversion of NFM and product selectivities. Reaction conditions: 0.3 g 13.5% CaO/MgO, 1.0 mmol NFM, 120 °C, 15 mL methanol.

To obtain kinetic information of the alcoholysis reaction, a plot of *ln*(*r*) versus *ln*(*c*(*NFM*)) was thus built (Figure 6). The resulting data were adjusted up to a kinetic behavior of about 0.73 order, which implies that the NFM concentration has a significant positive effect on the reaction rate. Moreover, it can be inferred that the excess of methanol in the catalytic system was necessary to ensure the methanol concentration remained essentially constant during the reaction process.

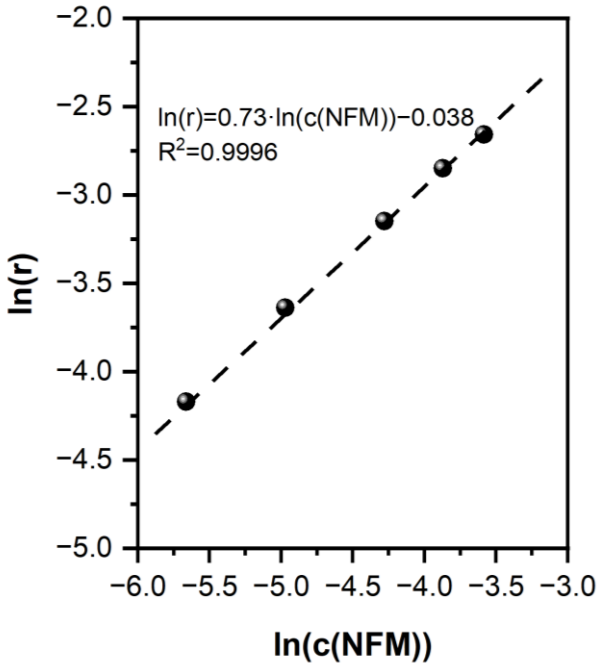


Figure 6. Linear plot of *ln*(*r*) versus *ln*(*c*(*NFM*)) resulting from the alcoholysis reaction of NFM. Reaction conditions: 0.3 g 13.5% CaO/MgO, NFM, 120 °C, 15 mL methanol.

The stability of the 13.5% CaO/MgO catalyst was also investigated at 120 °C. As shown in Figure 7, the reaction rate remained above 0.250 mmol·g^{-1}·h^{-1} with merely no

decrement over five successive cycles without regeneration, and the selectivities of MF and morpholine stayed constant at 100%. Such a result shows good stability and the potential for large-scale industrial application of the CaO/MgO catalysts.

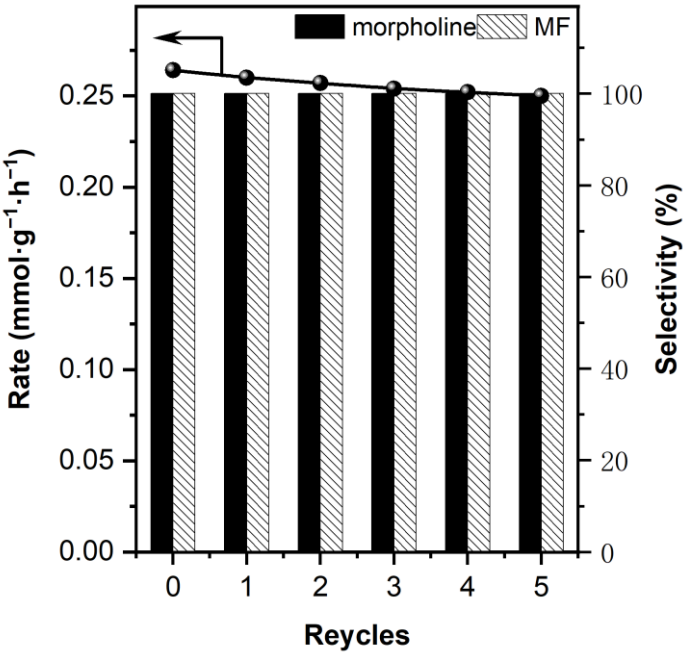


Figure 7. Stability of 13.5% CaO/MgO catalyst in the alcoholysis reaction of NFM during five repeated cycles. Reaction conditions: 0.3 g catalyst, 1.0 mmol NFM, 120 °C, 15 mL methanol.

As shown in Table 3, the alcoholysis activity of NFM showed significant variations in different alcohol solvents. NFM showed optimal alcoholysis reaction rate in methanol (Entry 1, 0.263 mmol·g^{-1}·h^{-1}), while its alcoholysis activity decreased continuously as the carbon chains of the alcohols gradually grew (Entry 2–4, the alcoholysis activities in ethanol, n-propanol, and n-butanol were 0.182, 0.151, and 0.128 mmol·g^{-1}·h^{-1}, respectively). Compared with other alcohols, the alkoxide anion formed in methanol has stronger basicity and smaller spatial resistance, which is more favorable to promote the alcoholysis reaction. Therefore, the alcoholysis reaction of formamides is more utilized to produce methyl formate rather than other formate esters.

Table 3. Alcoholysis rate of NFM and product selectivities in different alcohol solvents.

Entry	Solvent	Rate (mmol·g^{-1}·h^{-1})	Molar Selectivity (%)	
			Formate	Morpholine
1	methanol	0.263	100	100
2	ethanol	0.182	100	100
3	n-propanol	0.151	100	100
4	n-butanol	0.128	100	100

Reaction conditions: 120 °C, 0.3 g 13.5% CaO/MgO, 1.0 mmol NFM, 15 mL solvent, ~30% NFM conversion controlled by reaction time.

3. Materials and Methods

3.1. Catalyst Preparation

Bulk CaO and MgO were obtained by calcinating their corresponding acetate salts under a nitrogen atmosphere at 900 °C for 6 h. The CaO/MgO catalysts were prepared by (incipient wetness) impregnation with a solution of $Ca(CH_3COO)_2$ in deionized water. After the impregnation step, the samples were dried at 120 °C and calcined under a nitrogen

atmosphere at 900 °C for 6 h. These samples were classified as "x CaO/MgO", where "x" represents the mass fraction of CaO relative to the catalyst.

The other solid catalysts, except those specified, were purchased commercially directly and calcined at 300 °C for 4 h in a muffle furnace before use.

All the treated catalysts were placed in a glass dryer equipped with a calcium oxide desiccant before use to avoid moisture and CO_2 in the air affecting the activity of catalysts.

3.2. Catalyst Characterization

Specific surface areas (S_{BET}) of the catalysts were performed using a Micromeritics ASAP 2420 instrument using N_2 as an adsorption molecule by the multipoint Brunauer–Emmett–Teller (BET) method. Before testing, the catalysts were degassed under vacuum at 300 °C for 2 h.

X-ray powder diffraction (XRD) characterization was performed on an Empyrean X-ray diffractometer (PANalytical Corporation) equipped with a Cu K_α (λ = 1.5406 Å) radiation source in the 2θ scanning range 5–70° with generator voltage and tube current of 40 kV and 40 mA, respectively.

CO_2 temperature programmed desorption (CO_2-TPD) was carried out on a Tianjin Xianquan TP5080 multi-function adsorption instrument with a 10 μL quantitative loop. The sample was firstly heated in He flow (30 mL·min^{-1}) at 300 °C for 0.5 h to remove water and other impurities on the surface of catalyst. Once the sample was cooled down to 100 °C, the sample was treated in CO_2 flow (30 mL·min^{-1}) at 100 °C for another 30 min, and then in He flow until the baseline realized stable. Finally, CO_2-TPD was carried out with a heating rate of 10 °C·min^{-1} from 100 to 800 °C in He flow (30 mL·min^{-1}). The quantitative loop with known volume was used to calibrate the amount of CO_2 adsorbed on catalysts.

Transmission electron microscopy (TEM) images, high-resolution transmission electron microscopy (HRTEM) images, and elemental mapping results were acquired on JEM ARM200F transmission electron microscope with energy dispersive X-ray spectrometry (EDS) using an accelerating voltage of 200 kV. After the sample was dispersed in ethanol and ultrasonically treated for 0.5 h, the solution was dripped onto the ultra-thin copper mesh by glass capillary. Finally, the copper mesh was dried in a glass desiccator for 2 h at room temperature.

3.3. Catalytic Tests

Catalytic reactions of NFM were carried out in thick-wall glass tubes with vigorous stirring at a speed of 500 rpm. A certain amount of NFM was added into the glass tube with methanol to prepare the reactant solution with a certain mass concentration. The catalyst was then added to the NFM solution. The glass tube was sealed by Teflon caps and heated to the reaction temperature by an IKA-heated magnetic stirrer. After each experiment, the catalyst was separated by gravity filtration from the mixed solution of products using a nylon-66 filter (0.22 μm porosity and 4 cm diameter). The so-recovered catalyst was then rinsed with 20 mL pure methanol, and the obtained filtrate was chemically analyzed to find the quantitative analysis of reactant conversion and product selectivity. The concentrations of NFM and alcoholysis products were quantified by Agilent 7890B GC equipped with an FID detector and LZP35 capillary column. For that, aliquots of the catalyst-free liquid were collected using a syringe assembled with a filter and injected directly into the chromatographic analyzers.

The conversion of NFM and selectivities of MF and morpholine on a molar basis were calculated by the following formulas:

$$X_{NFM} = \frac{C_{NFM}^{in} - C_{NFM}^{out}}{C_{NFM}^{in}} \times 100\%$$

$$S_{MF} = \frac{C_{MF}^{out}}{C_{NFM}^{in} - C_{NFM}^{out}} \times 100\%$$

$$S_{morpholine} = \frac{C^{out}_{morpholine}}{C^{in}_{NFM} - C^{out}_{NFM}} \times 100\%$$

where X_{NFM} is the conversion of NFM, %; S_{MF} and $S_{morpholine}$ are the selectivities of MF and morpholine, respectively, %; and C_n is the molar concentration of NFM, MF, or morpholine, mol/L, based on GC analysis results.

4. Conclusions

In this study, a series of CaO/MgO catalysts was prepared by impregnation and used in an alcoholysis reaction to synthesize MF by using CO_2-derived formamides and green methanol. It was found that the alcoholysis rate of NFM on 13.5% CaO/MgO could reach 0.263 mmol·g^{-1}·h^{-1}, which was ca. 1.5 times higher than that of bulk CaO catalyst, and achieved 94.5% conversion of N-formylmorpholine and 100% selectivity of MF in methanol at 120 °C. The structural characterization results and kinetic studies indicate that CaO can be well dispersed on the MgO support and the strong basic sites are the intrinsic active species of CaO/MgO catalysts. Moreover, CaO/MgO catalysts performed good stability and recyclability. All the results from this research point out that the development of solid base catalysts with a high density of base sites is the key to achieving the effective and sustainable preparation of MF from the alcoholysis reaction of formamides. Currently, we are also developing new processes for the preparation of methyl formate from carbon dioxide, hydrogen, and amines (recyclable raw materials).

Author Contributions: Conceptualization, X.H. and G.X.; methodology, X.H. and X.G.; validation, X.H.; formal analysis, X.H.; investigation, X.H. and X.G.; data curation, X.H.; writing—original draft preparation, X.H.; writing—review and editing, G.X., R.X., Y.W. and X.L.; visualization, X.H.; All authors have read and agreed to the published version of the manuscript.

Funding: This research received no external funding.

Data Availability Statement: The data presented in this study are available on request from the corresponding author.

Acknowledgments: The authors thank Kangyu Liu and Xuandong Liu for their guidance and support.

Conflicts of Interest: The authors declare no conflict of interest.

References

1. Bertau, M.; Offermanns, H.; Plass, L.; Schmidt, F.; Wernicke, H.-J. *Methanol: The Basic Chemical and Energy Feedstock of the Future*; Springer: Berlin, Germany, 2014; Volume 1.
2. Haynes, A. Chapter 1—Catalytic Methanol Carbonylation. In *Advances in Catalysis*; Gates, B.C., Knözinger, H., Eds.; Academic Press: New York, NY, USA, 2010; Volume 53, pp. 1–45.
3. Ren, Z.; Lyu, Y.; Song, X.; Ding, Y. Review of Heterogeneous Methanol Carbonylation to Acetyl Species. *Appl. Catal. A* **2020**, *595*, 117488. [CrossRef]
4. Guerreiro, E.D.; Gorriz, O.F.; Larsen, G.; Arrúa, L.A. Cu/SiO_2 Catalysts for Methanol to Methyl Formate Dehydrogenation. *Appl. Catal. A* **2000**, *204*, 33–48. [CrossRef]
5. Wu, S.; Sun, W.; Wang, X.; Zhao, J.; Li, Y.; Quan, Y.; Ren, J. Insights into the Crucial Role of a Zn Promoter for Methanol Dehydrogenation to Methyl Formate over Cu(111) Catalysts. *Phys. Chem. Chem. Phys.* **2022**, *24*, 22661–22669. [CrossRef] [PubMed]
6. Gao, P.; Li, S.; Bu, X.; Dang, S.; Liu, Z.; Wang, H.; Zhong, L.; Qiu, M.; Yang, C.; Cai, J.; et al. Direct Conversion of CO_2 into Liquid Fuels with High Selectivity over a Bifunctional Catalyst. *Nat. Chem.* **2017**, *9*, 1019–1024. [CrossRef]
7. Wei, J.; Yao, R.; Han, Y.; Ge, Q.; Sun, J. Towards the Development of The Emerging Process of CO_2 Heterogenous Hydrogenation into High-Value Unsaturated Heavy Hydrocarbons. *Chem. Soc. Rev.* **2021**, *50*, 10764–10805. [CrossRef]
8. Liu, Q.; Wu, L.; Jackstell, R.; Beller, M. Using Carbon Dioxide as a Building Block in Organic Synthesis. *Nat. Commun.* **2015**, *6*, 5933. [CrossRef]
9. Jessop, P.G.; Hsiao, Y.; Ikariya, T.; Noyori, R. Catalytic Production of Dimethylformamide from Supercritical Carbon Dioxide. *J. Am. Chem. Soc.* **2002**, *116*, 8851–8852. [CrossRef]
10. Jessop, P.G.; Hsiao, Y.; Ikariya, T.; Noyori, R. Homogeneous Catalysis in Supercritical Fluids: Hydrogenation of Supercritical Carbon Dioxide to Formic Acid, Alkyl Formates, and Formamides. *J. Am. Chem. Soc.* **1996**, *118*, 344–355. [CrossRef]

11. Kröcher, O.; Köppel, R.A.; Baiker, A. Highly Active Ruthenium Complexes with Bidentate Phosphine Ligands for the Solvent-Free Catalytic Synthesis of N,N-dimethylformamide and Methyl Formate. *Chem. Commun.* **1997**, *5*, 453–454. [CrossRef]
12. Zhang, L.; Han, Z.; Zhao, X.; Wang, Z.; Ding, K. Highly Efficient Ruthenium-Catalyzed N-Formylation of Amines with H_2 and CO_2. *Angew. Chem. Int. Ed.* **2015**, *54*, 6186–6189. [CrossRef]
13. Chong, C.C.; Kinjo, R. Hydrophosphination of CO_2 and Subsequent Formate Transfer in the 1,3,2-Diazaphospholene-Catalyzed N-Formylation of Amines. *Angew. Chem. Int. Ed.* **2015**, *54*, 12116–12120. [CrossRef] [PubMed]
14. Cui, X.; Zhang, Y.; Deng, Y.; Shi, F. Amine Formylation via Carbon Dioxide Recycling Catalyzed by a Simple and Efficient Heterogeneous Palladium Catalyst. *Chem. Commun.* **2014**, *50*, 189–191. [CrossRef]
15. Li, R.; Zhao, Y.; Wang, H.; Li, D.; Wu, Y.; Zhang, H.; Tang, M.; Liu, Z. Ionic Liquid-Promoted Formylation of N(sp2)-Heteroarenes with CO_2/H_2 over Pd/C. *ACS Sustain. Chem. Eng.* **2021**, *9*, 2507–2514. [CrossRef]
16. Wang, G.; Jiang, M.; Ji, G.; Sun, Z.; Ma, L.; Li, C.; Du, H.; Yan, L.; Ding, Y. Highly Efficient Heterogeneous Pd@Pops Catalyst for the N-Formylation of Amine and CO_2. *Catalysts* **2021**, *11*, 220. [CrossRef]
17. Liu, J.; Guo, C.; Zhang, Z.; Jiang, T.; Liu, H.; Song, J.; Fan, H.; Han, B. Synthesis of Dimethylformamide from CO_2, H_2 and Dimethylamine over Cu/ZnO. *Chem. Commun.* **2010**, *46*, 5770–5772. [CrossRef]
18. Bi, Q.Y.; Lin, J.D.; Liu, Y.M.; Xie, S.H.; He, H.Y.; Cao, Y. Partially Reduced Iridium Oxide Clusters Dispersed on Titania as Efficient Catalysts for Facile Synthesis of Dimethylformamide from CO_2, H_2 And Dimethylamine. *Chem. Commun.* **2014**, *50*, 9138–9140. [CrossRef]
19. Fitzgerald, L.S.; O'Duill, M.L. A Guide to Directing Group Removal: 8-Aminoquinoline. *Chem. Eur. J.* **2021**, *27*, 8411–8436. [CrossRef] [PubMed]
20. Kamachi, T.; Siddiki, S.M.A.H.; Morita, Y.; Rashed, M.N.; Kon, K.; Toyao, T.; Shimizu, K.-i.; Yoshizawa, K. Combined Theoretical and Experimental Study on Alcoholysis of Amides on CeO_2 Surface: A Catalytic Interplay between Lewis Acid and Base Sites. *Catal. Today* **2018**, *303*, 256–262. [CrossRef]
21. Li, H.; Guo, H.; Su, Y.; Hiraga, Y.; Fang, Z.; Hensen, E.J.M.; Watanabe, M.; Smith, R.L., Jr. N-formyl-stabilizing Quasi-Catalytic Species Afford Rapid and Selective Solvent-Free Amination of Biomass-Derived Feedstocks. *Nat. Commun.* **2019**, *10*, 699. [CrossRef]
22. Deguchi, T.; Xin, H.-L.; Morimoto, H.; Ohshima, T. Direct Catalytic Alcoholysis of Unactivated 8-Aminoquinoline Amides. *ACS Catal.* **2017**, *7*, 3157–3161. [CrossRef]
23. Siddiki, S.M.A.H.; Touchy, A.S.; Tamura, M.; Shimizu, K.-i. Versatile And Sustainable Alcoholysis Of Amides By A Reusable CeO_2 Catalyst. *RSC Adv.* **2014**, *4*, 35803–35807. [CrossRef]
24. Avhad, M.R.; Marchetti, J.M. A Reviewon Recent Advancement in Catalytic Materials for Biodiesel Production. *Renew. Sustain. Energy Rev.* **2015**, *50*, 696–718. [CrossRef]
25. Wu, H.; Zhang, J.; Wei, Q.; Zheng, J.; Zhang, J. Transesterification of Soybean Oil to Biodiesel Using Zeolite Supported Cao as Strong Base Catalysts. *Fuel Process. Technol.* **2013**, *109*, 13–18. [CrossRef]
26. Simanjuntak, F.S.H.; Kim, T.K.; Lee, S.D.; Ahn, B.S.; Kim, H.S.; Lee, H. Cao-Catalyzed Synthesis of Glycerol Carbonate from Glycerol and Dimethyl Carbonate: Isolation and Characterization of An Active Ca Species. *Appl. Catal. A* **2011**, *401*, 220–225. [CrossRef]
27. He, X.; Wen, X.; Wu, K.; Liu, H. Sustainable Synthesis of Vinyl Methyl Ether From Biomass-Derived Ethylene Glycol Dimethyl Ether over Solid Base Catalysts. *Green Chem.* **2021**, *23*, 6625–6631. [CrossRef]
28. Kouzu, M.; Kasuno, T.; Tajika, M.; Sugimoto, Y.; Yamanaka, S.; Hidaka, J. Calcium oxide as a solid base catalyst for transesterification of soybean oil and its application to biodiesel production. *Fuel* **2008**, *87*, 2798–2806. [CrossRef]
29. Zul, N.A.; Ganesan, S.; Hamidon, T.S.; Oh, W.-D.; Hussin, M.H. A review on the utilization of calcium oxide as a base catalyst in biodiesel production. *J. Environ. Chem. Eng.* **2021**, *9*. [CrossRef]
30. Li, Z.; Niu, S.; Han, K.; Li, Y.; Wang, Y.; Lu, C.; Cheng, S. Investigation into influences of methanol pre-adsorption on CaO(100) surface in transesterification for biodiesel production with molecular simulation. *Appl. Catal. A* **2021**, *609*. [CrossRef]
31. Yan, S.; Lu, H.; Liang, B. Supported CaO Catalysts Used in the Transesterification of Rapeseed Oil for the Purpose of Biodiesel Production. *Energy Fuels* **2007**, *22*, 646–651. [CrossRef]

Disclaimer/Publisher's Note: The statements, opinions and data contained in all publications are solely those of the individual author(s) and contributor(s) and not of MDPI and/or the editor(s). MDPI and/or the editor(s) disclaim responsibility for any injury to people or property resulting from any ideas, methods, instructions or products referred to in the content.